Seed layer induced (002) crystallographic texture in NiAl underlayers

Li-Lien Lee, David E. Laughlin, and David N. Lambeth
Data Storage Systems Center, Carnegie Mellon University, Pittsburgh, Pennsylvania 15213

The magnetic properties of Co alloy thin films are strongly dependent on their crystallographic texture and microstructure which in turn can be controlled by the texture of the underlayer. For Co alloy longitudinal recording media with Cr underlayers, it is desirable to have (002) textured Cr underlayers. Since NiAl has the $B2$ structure and has a lattice constant similar to that of Cr, NiAl has the potential to be an alternative underlayer to Cr. However, the (002) crystallographic texture of the NiAl films is difficult to obtain. It is found that the (002) texture in NiAl underlayers can be achieved by employing a seed layer of either (002) textured Cr or MgO. Because of the improved texture a significant increase of the in-plane coercivity in CoCrPt/NiAl films was obtained. © *1996 American Institute of Physics.* [S0021-8979(96)07908-4]

NiAl is an ordered phase with the $B2$ structure. It has a similar crystal structure and lattice constant as that of Cr. It has been shown by the authors that sputter-deposited NiAl films can be used as underlayers for HCP Co alloy longitudinal recording media.[1,2] Sputter deposited NiAl underlayers tend to induce good in-plane c-axis texture in the overlying Co films through the NiAl (112) preferred oriented film planes. An often asked question is: can the crystallographic texture of the NiAl underlayer be altered?

One of the frequently sought after crystallographic textures for Cr underlayers is (002). It has been argued by Zhu[3] that the (002) textured Cr underlayers may render a high signal-to-noise ratio in the HCP Co alloy thin film recording media. Since NiAl and Cr are structurally similar, a (002) textured NiAl may impart a similar benefit. We have tried to raise the substrate temperature during the sputtering of NiAl, a practice often used to achieve the (002) texture in Cr. However, this approach fails to produce the (002) texture in the NiAl film. Other means have to be found. A simple solution to this is by making use of a proper seed layer. A seed layer (sometimes called a precoating) is a thin-film layer that is deposited between the substrate and the underlayer. Seed layers are used for (1) the facilitation of infrared heating of glass substrates, (2) the modification of the topography of the disk substrates for tribological purpose, and (3) inducing preferred crystallographic texture to underlayers.

For longitudinal recording media, seed layers such as Al,[4] Ti,[5] Ni_3P, $TiSi_2$, Cr, C,[6] Ta, W, and Zr[7] have been used. Varying degrees of success have been reported, however, the industry is still in the process of searching for a better seed layer. Because of the similarity in crystal structures of NiAl and Cr, employment of a (002) Cr seed layer, which can be achieved by sputter depositing on to a heated substrate, is another approach to inducing the crystallographic texture of NiAl to (002). Another kind of seed layer which may do the same is MgO.

MgO is an ionic crystal with the $B1$ (NaCl-type) crystal structure with a lattice constant of 0.421 nm. It has been shown by Nakamura and Futamoto[8] that a Cr film deposited on a single-crystal (002) MgO tends to have its (002) plane lying parallel to the film plane due to heteroepitaxial growth. It is easy to obtain a sputter-deposited MgO film with a (002) texture because the (002) plane has the lowest surface energy.[9] Here, the authors have found that, similar to Cr, NiAl deposited on a MgO seed layer can have the (002) texture.

All films were deposited by rf diode sputtering. The deposition conditions were the same as that of the previous papers by the authors.[1,2] The MgO films were deposited by rf sputtering of a 99.95 at. % pure MgO bulk target and the deposition rate was 4 nm/min. The HCP Co alloy films used in this study were obtained by sputtering from a CoCr target

TABLE I. The in-plane magnetic properties of the CoCrPt (40 nm)/NiAl(100 nm) films on MgO seed layers of various thickness.

MgO thickness	H_c (Oe)	S^*	S	Mrt (memu/cm^2)
0nm	1862	0.87	0.84	1.4
2nm	2558	0.92	0.86	1.1
5nm	2811	0.92	0.87	1.2
8nm	3283	0.92	0.88	1.1
10nm	3238	0.91	0.87	1.0
20nm	3236	0.86	0.84	1.0
50nm	3182	0.82	0.87	1.0

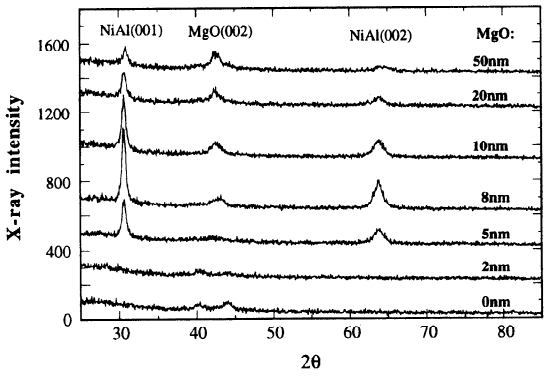

FIG. 1. X-ray diffraction spectra of CoCrPt(40 nm)/NiAl(100 nm) films on various thicknesses of MgO seed layers.

 0021-8979/96/79(8)/4902/3/$10.00

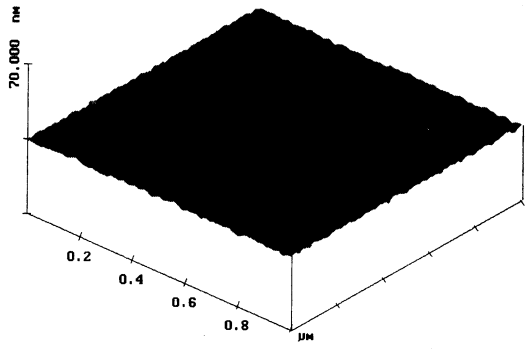

(a) NiAl,100nm/MgO,10nm/glass

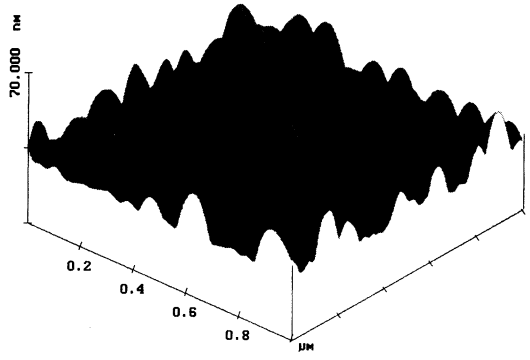

(b) NiAl,100nm/MgO,20nm/glass

FIG. 2. AFM surface plots of 100 nm NiAl films with MgO seed layers of (a) 10 nm and (b) 20 nm on smooth glass substrates.

with bonded Pt chips. Substrates were biased at -100 V with respect to the target during the deposition of CoCrPt films. EDX analysis of the magnetic CoCrPt film determined the composition to be $CoCr_{10}Pt_{18}$. Smooth glass substrates were used. Film thicknesses were determined by profilometry. Surface morphology of the films were checked by atomic force microscopy (AFM). Transmission electron microscopy (TEM) was performed on studying the films' plane-view microstructure. In-plane magnetic properties were measured by vibrating sample magnetometry (VSM). Crystallographic textures were studied by x-ray diffractometry with Cu $K\alpha$ radiation.

TABLE II. The in-plane magnetic properties of the 40 nm CoCrPt films on 100 nm NiAl, 100 nm Cr, and 100 nm NiAl/10 nm Cr underlayers.

Underlayer	H_c (Oe)	S^*	S	Mrt (memu/cm^2)
NiAl	2221	0.79	0.81	0.81
Cr	2228	0.74	0.85	0.83
NiAl/Cr	3153	0.78	0.85	0.84

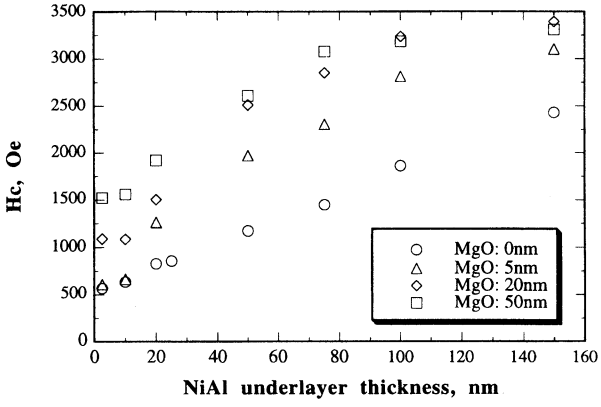

FIG. 3. Coercivity values of the 40-nm-thick CoCrPt vs their NiAl underlayer thickness for MgO seed layers of 0, 5, 10, 20 nm thick.

Table I lists the VSM measurements of the 40-nm-thick CoCrPt films on 100 nm NiAl underlayers on MgO seed layers of various thicknesses. The coercivity increases rapidly and then levels off as the MgO seed layer thickens. The maximum coercivity of 3280 Oe occurs at a MgO thickness of 8 nm. The crystallographic texture of these 40 nm CoCrPt/100 nm NiAl films on MgO seed layers revealed by x-ray diffraction spectra are plotted in Fig. 1. The (002) MgO peak continuously becomes stronger as the MgO layer thickens. However, the intensity of the (002) NiAl peak is not proportional to the MgO thickness. The maximum coercivity film in Table I corresponds to the film with the strongest (002) NiAl crystallographic texture.

AFM studies of the films showed little increase in surface roughness as the MgO seed layer is increased from 2 to 10 nm. However, there is a dramatic increase of the surface roughness as the MgO seed layer reaches 20 nm which is believed to be the main cause for the apparent deterioration of the epitaxy between NiAl and MgO. Figure 2 shows the AFM surface topography plots of 100 nm NiAl films on 10 and 20 nm MgO seed layers on glass substrates. A 20 nm MgO seed layer can roughen the film considerably to form

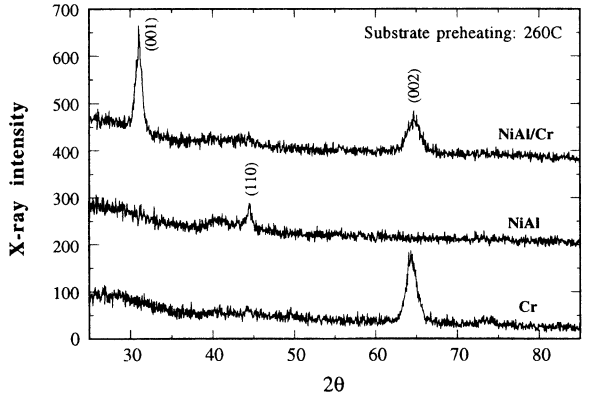

FIG. 4. X-ray diffraction spectra of the CoCrPt(40 nm)/Cr(100 nm) film and CoCrPt(40 nm)/NiAl(100 nm) films with and without a 10 nm Cr seed layer. These films were all deposited with 260 °C substrate preheating.

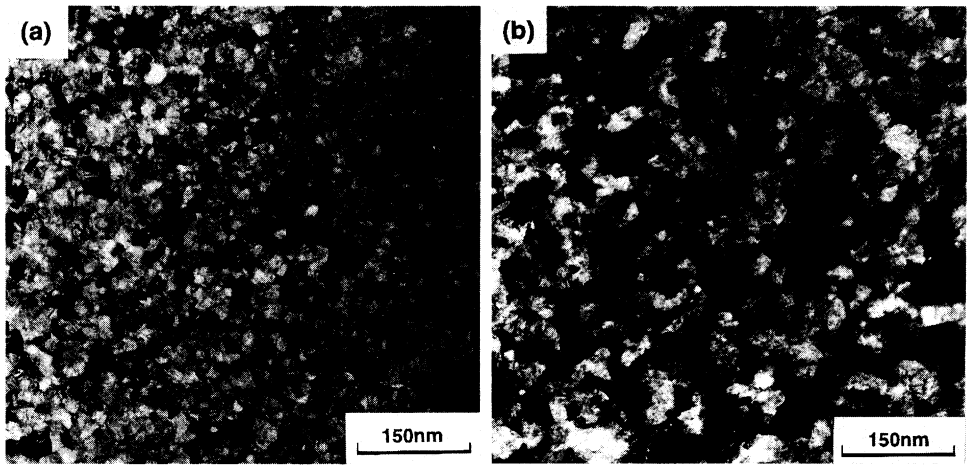

FIG. 5. Bright-field TEM micrographs of CoCrPt(40 nm)/NiAl(100 nm) films (a) on a 5 nm MgO seed layer and (b) on a 10 nm Cr seed layer.

surface bumps of up to ~150 nm in diameter and ~25 nm in height. Because a low flying height is necessary for future high-density recording media, this surface roughening may be problematic. On the other hand, to avoid the stiction of the head slider to the smooth disk the surface of the disk substrate is generally roughened by mechanical and/or chemical texturing. For glass disks, a sputtered texture is often used.[10] With the MgO seed layer the roughness can be tailored by controlling the MgO layer thickness or fine tuning the sputtering process.

Figure 3 is a plot of four sets of coercivity data of the 40-nm-thick CoCrPt films versus their NiAl underlayer thicknesses for MgO seed layers of 0, 5, 20, and 50 nm.

Likewise, a 10 nm Cr seed layer when prepared on a 260 °C preheated substrate induces (002) texture in a subsequent NiAl layer. Figure 4 plots the x-ray diffraction spectra of 40 nm CoCrPt/100 nm NiAl films with and without a 10 nm Cr seed layer and a 40 nm CoCrPt/100 nm Cr film. For comparison, these films were all deposited onto 260 °C preheated substrates. The substrate preheating helps to bring out the (002) texture in the NiAl underlayer with a Cr seed layer as well as the standard pure Cr underlayer. However, no (002) peak is observed in the film with only the pure NiAl underlayer. Table II lists the in-plane bulk magnetic properties of the specimens depicted in Fig. 4. It shows the coercivity of the CoCrPt film on the NiAl underlayer is significantly increased due to the incorporation of the Cr seed layer, similar to the MgO seed layer. However, lower coercivity squareness and $M_r t$ were observed in the film with a Cr seed layer. With a similar (002) texture, the NiAl underlayer appears to induce a higher coercivity in the CoCrPt film than the Cr underlayer.

Figure 5 compares the TEM bright-field micrographs of 40 nm CoCrPt/100 nm NiAl films on 5 nm MgO and 10 nm Cr seed layers. Although these plane-view micrographs show overlapping NiAl and Co grains, it is obvious that the grain size of the film with a Cr seed layer is more than twice the grain size (180 Å) of the film with a MgO seed layer.

In summary, seed layers of Cr and MgO which can induce the (002) crystallographic texture in the NiAl underlayers were shown to be beneficial to the in-plane coercivity of the CoCrPt films. While Cr seed layers require substrate heating, MgO seed layers do not. Therefore, films on a MgO seed layer have finer grains. Surface roughness can also be tailored by using a MgO layer which can provide sputtered texture to smooth substrates to reduce the stiction of the head to the smooth disk.

This work was supported in part by the DSSC of CMU under a NSF Grant No. ECD-8907068 and an ARPA Contract No. MDA972-93-1-0009. The government has certain rights to this material.

[1] L.-L. Lee, D. E. Laughlin, and D. N. Lambeth, IEEE Trans. Magn. **MAG-30**, 3951 (1994).
[2] L.-L. Lee, D. E. Laughlin, and D. N. Lambeth, IEEE Trans. Magn. **MAG-31**, 2728 (1995).
[3] J. Zhu and X. Ye, Digests of Intermag 95, Paper FA03, (1995).
[4] H. S. Chang, K. H. Shin, T. D. Lee, and J. K. Park, IEEE Trans. Magn. **MAG-31**, 2731 (1995).
[5] T. Kogure and S. Katayama, J. Appl. Phys. **67**, 4701 (1990).
[6] X. Tang, B. Reed, and R. Zubeck, IEEE Trans. Magn. **MAG-30**, 3963 (1994).
[7] H. Kataoka, T. Kanbe, H. Kashiwase, E. Fujita, Y. Yashisa, and K. furusawa, Intermag 95 Paper BC03, IEEE Trans. Magn. **MAG-31**, 2734 (1995).
[8] A. Nakamura and M. Futamoto, Jpn. J. Appl. Phys. **32**, L1414 (1993).
[9] P. W. Tasker, Adv. Ceram. **10**, 176 (1984).
[10] M. Mirzamaani and C. V. Jahnes, IEEE Trans. Magn. **MAG-28**, 3090 (1992).